



Advancements in Rayleigh scattering thermometry by means of structured illumination

Elias Kristensson, Andreas Ehn, Joakim Bood*, Marcus Aldén

Division of Combustion Physics, Lund University, Box 118, Lund S-221 00, Sweden

Available online 27 June 2014

Abstract

Laser-induced Rayleigh scattering is commonly employed for two-dimensional temperature measurements and offers benefits such as high accuracy, easily interpreted data and low experimental complexity. Yet the approach suffers from an interference often referred to as stray light, an umbrella term used for all spurious light being detected. As Rayleigh scattering is an elastic scattering phenomenon, distinguishing between stray light and the signal of interest is not straightforward. In high-temperature environments, Rayleigh signals are weak due to low molecular densities, which make stray light interferences particularly cumbersome, impairing both the reliability and accuracy of Rayleigh thermometry, especially when applied in harsh combustion environments. In this paper we present an experimental solution to greatly mitigate this issue. The method, Structured Laser Illumination Planar Imaging (SLIPI), employs an intensity modulated laser light sheet to add a recognizable signature to the signal photons. This unique signature allows utilization of a post-processing algorithm that isolates and extracts the desired Rayleigh signal, thereby minimizing measurement uncertainties caused by stray light. The fidelity of the proposed method is first verified by comparing with conventional Rayleigh thermometry under ideal, i.e., stray light-free, measurement conditions. The technique is then employed under more realistic measurement conditions, where the results conclusively illustrate that the current operating range for Rayleigh thermometry can be increased significantly by means of SLIPI.

© 2014 The Combustion Institute. Published by Elsevier Inc. All rights reserved.

Keywords: Rayleigh scattering; Thermometry; Two-dimensional imaging; Stray light; Structured illumination

1. Introduction

Temperature is one of the most important measurement parameters of combustion systems and, over the years, several laser-based techniques (preferred for being non-intrusive) have been developed to access this information. Two-line

atomic fluorescence (TLAF) aims at sensing the relative population of two atomic energy states to deduce the gas temperature from the Boltzmann distribution [1]. This method may provide two-dimensional (2-D) information if combined with the laser light sheet technique [2,3]. However, the use of TLAF is limited in many practical applications, since it requires two tunable laser systems and a seeded fluorescing (non-combusting) species properly added to the flame, which might be affected by the combustion itself.

* Corresponding author. Fax: +46 46 222 45 42.

E-mail address: joakim.bood@forbrf.lth.se (J. Bood).

Atomic indium, for example, is oxidized under fuel-lean conditions, which reduces the fluorescence intensity [4]. Raman scattering can also be used for thermometry and has the added benefit of being species-specific [5], yet the method suffers from very low signal levels and is therefore hardly applicable for 2-D imaging. Coherent anti-Stokes Raman spectroscopy (CARS) provides very accurate temperature readings, but is, in principle, restricted to point measurements [6]. 1D-CARS has been demonstrated, but the setup relies on a combination of a femtosecond and a picosecond laser system [7], thus making it a very expensive and complex approach. In recent years, laser-induced phosphorescence has emerged as an alternative method to measure temperature [8], but is, at present, mostly suited for wall-temperature readings [9]. This is due to the need for seeding particles and the low particle density in high temperature regions leads to insufficient signal levels [10]. In addition, adequate phosphors for flame temperatures are not available.

Laser-induced Rayleigh scattering (LRS) has long been employed for thermometry in combustion and is, in many ways, a very attractive method for this purpose, at least in theory; it does not require any seeder, it can provide 2-D information in all regions of the flame, signal levels are relatively weak but usually sufficient for measurements in high-temperature environments, and the data evaluation is, in most cases, straightforward [11, 12]. Exploiting these benefits is, however, often very challenging in practical applications.

Laser-induced Rayleigh scattering is an elastic scattering method that takes advantage of changes in number density to assess the gas temperature; as the number density drops due to an elevation in temperature, for fixed pressure, the Rayleigh scattering intensity reduces accordingly. Under ideal measurement conditions, the main uncertainty of LRS concerns variations in the scattering cross-section due to variations in the composition of the probed volume. For measurements in premixed flames, such variations can be minimized by judiciously selecting the fuel and oxidizer flows [5,13]. However, in most practical measurement situations, e.g. in engines, gas turbines, or other combustion environments where a laser light beam passes through optical windows, the primary source of error and limiting factor for LRS is instead related to the detection of stray light - an interference comprising all spurious light reaching the camera [14]. Although most imaging techniques share this limitation in one way or another, LRS is unfortunately especially sensitive to stray light contamination. The reason for this is twofold: (1) the Rayleigh signal is not shifted in wavelength, which precludes the use of optical filters for suppression of, for example, laser light reflections, and (2) Rayleigh scattering is relatively weak compared to scattering from e.g. dust, particles, and

droplets (i.e., Mie scattering), which greatly exceeds the Rayleigh scattered intensity. In addition, implementing LRS for thermometry in combustion applications adds further experimental complexity; the high temperature, and thereby low number density, leads to a low signal-to-noise ratio (S/N). All intensity contributions stemming from other sources - reflections, flame emission, Mie scattering, etc. - therefore greatly affect the fidelity of the measurement, and it can be stated that the accuracy of the technique relies on the ability to either (1) precisely subtract a representative 2-D background intensity field or (2) prevent the creation of this undesired light. Unfortunately neither solution is straightforward in practical applications. For example, one of the most well-known approaches to estimate the stray light component nowadays involves filling the experimental region with Helium, which has a negligible Rayleigh scattering cross-section, and to repeat the laser measurement. The detected signal is then subtracted from the previously acquired LRS data [15]. Although providing an estimate of the stray light component, the method adds measurement complexity and can only be implemented in enclosed environments. In addition, variations in stray light, due to e.g., sample fluctuations, cannot be compensated for.

In an attempt to improve the accuracy and reliability of LRS, Miles and Lempert developed a method to experimentally suppress stray light [16]. Their approach, which later was given the name filtered Rayleigh scattering (FRS), takes advantage of the fact that solid surfaces and particles are, or can be considered, static compared to gas molecules and will therefore not give rise to any considerable Doppler broadening. By tuning a single-mode laser to match an extremely narrow absorption filter the authors demonstrated the possibility to only detect Doppler-shifted light, i.e., primarily photons scattered off gas molecules. Even though the scheme offers the unique possibility to discard diffuse laser-induced backgrounds as well as scattering from particles in the probe volume, FRS suffers from some inherent drawbacks that limit its use in practical applications. Above all, much of the signal is blocked by the atomic filter, which decreases the signal-to-noise ratio. Further, FRS has to be performed with rather specialized equipment, where the wavelength of a narrowband laser has to match the atomic filter exactly. In addition, the temperature evaluation routine must take into account, not only the species-specific Rayleigh cross-sections in each volume, but also the spectral shape of the emission, which is largely dependent on pressure and species number densities. The S6 model, developed by Tenti and co-workers, can be used to determine the Doppler line profile [17]. However, the model assumes merely diatomic molecules.

Motivated by these issues related to the LRS technique, we have developed an alternative, less experimentally complicated, approach to mitigate stray light arising from laser-induced backgrounds. The proposed approach is based on a laser light sheet technique known as SLIPI (Structured Laser Illumination Planar Imaging), developed and applied primarily for spray visualization [18]. The technical detail differentiating conventional laser light sheet imaging and SLIPI is that the latter provides means to evaluate the background intensity that is present in the actual recording. This feature is important since the background in an LRS measurement of a combustion event is not constant, neither temporally nor spatially, and can therefore not be attained at any other occasion. Note, however, that in contrast to FRS, the method cannot differentiate between Rayleigh and Mie scattering that originates from the probe volume. As will be demonstrated, failure in removing the background intensity in an LRS measurement will lead to inaccuracies in the evaluated temperature.

In this paper, a general description of the SLIPI technique is first provided and thereafter the experimental setup employed in the current study is presented. Finally, the temperature realizations obtained using either conventional- or SLIPI LRS are compared and discussed.

2. Structured Laser Illumination Planar Imaging, SLIPI

SLIPI is the unification of laser light sheet imaging and structured illumination (primarily used within microscopy [19]). The technique has, so far, been applied mainly for spray visualization to suppress multiply scattered light [18]. However, in terms of image characteristics, multiply scattered light and stray light are identical, suggesting that SLIPI could be utilized to suppress the latter source of error as well.

With SLIPI, the laser light sheet is first guided through a transmission Ronchi grating before it is directed into the sample. The grating leaves a structural imprint on the laser light sheet profile (Fig. 1) – a sinusoidal modulation with a well-defined spatial frequency and phase. Photons that are scattered from the laser light sheet directly to the camera (signal photons) preserve this structure whereas all background sources appear as offsets (sharp or diffuse) in the recorded image. The different characteristics of the two image components permit the removal of the unwanted offsets, which can be accomplished in two ways. Common practice is to record three modulated laser light sheet images, between which the modulation is phase-shifted 120 degrees [19]. An offset-corrected image (I_s) is then obtained by calculating

$$I_s = \sqrt{(I_0 - I_{120})^2 + (I_0 - I_{240})^2 + (I_{120} - I_{240})^2}, \quad (1)$$

where I_X is a modulated laser light sheet image and the subscript X denotes the spatial phase.

Although less common, the background can also be removed from a single acquisition, at the cost of spatial resolution. Berrocal et al. demonstrated such a method, which takes advantage of the fact that only signal photons appear with the spatial frequency and phase set by the Ronchi grating – all other image components must have arisen from interfering sources [20]. We incorporate a similar methodology here but our calculations are instead based on lock-in detection (in the spatial domain) to isolate and extract those spatial frequency components that share the characteristics set by the Ronchi grating. In short, the approach first extracts the modulation frequency, k_y , which is readily accessible in the Fourier transform, see Fig. 1. Based on this value, two reference signals – sinusoidal vectors, phase-shifted 90 degrees from each other – are constructed and multiplied with each column of the acquired LRS image. Because of the precise match in spatial frequency, this multiplication results in (1) a demodulation of the modulated part of the column data and (2) a shift in frequency of all non-modulated (background) components. One could imagine that the approach rearranges the components in reciprocal space, placing unwanted spatial frequencies far from the origin and the desired k_y (i.e., the local amplitude of the modulation) at its center. Low-pass filtering the new (rearranged) data permits access to only those image components in the LRS image that were modulated with a spatial frequency of k_y . The approach is described in greater detail in [21] and the fundamental principles of lock-in-detection are found in [22]. The main drawback with the method is the loss of spatial resolution associated with the low-pass filter, which smoothens image gradients. For ensemble-averaged imaging, high spatial structures are smeared out, and the selection of modulation frequency is not critical. However, for single-shot applications, where sharper image gradients are expected, it is advised to choose a modulation frequency (k_y) high enough to maintain an adequate spatial resolution. Although, if spatial resolution cannot be sacrificed, it is possible to incorporate structured illumination in the more traditional fashion instead, according to Eq. (1), which does not rely on low-pass filtering but, on the downside, requires three lasers for single-shot imaging. Regardless of the methodology used to suppress the stray light – multiple acquisitions or lock-in detection – it is important to note that the suppression occurs in the post-processing of the data. Hence, a LRS measurement that is completely over-

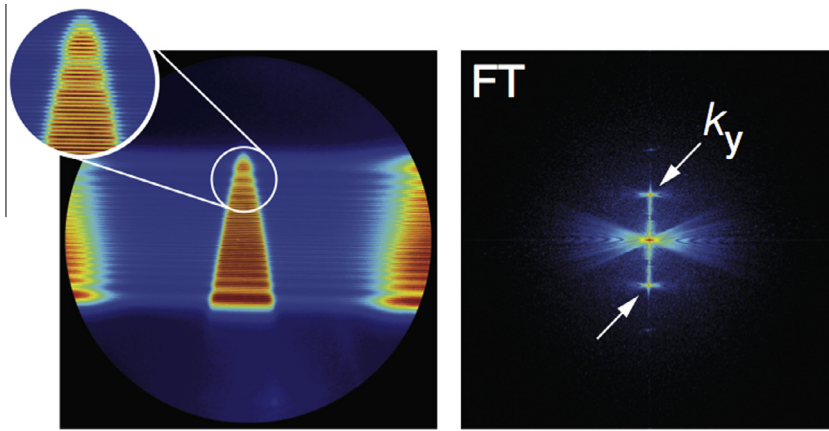


Fig. 1. An LRS image of a Bunsen-type flame using a modulated laser light sheet, together with its 2-D Fourier transform (logarithmic intensity scale). All light scattered from the laser light sheet carries the superimposed modulation and this characteristics will differentiate them from stray light. The modulated component (needed in the post-processing) is easily identified in the Fourier transform, indicated by white arrows.

whelmed by background interferences cannot be restored by means of SLIPI; issues related to the finite dynamic range of the detector still remain.

3. Experimental setup

The main restricting factor for combining SLIPI and LRS concerns the laser light power required to achieve a sufficient Rayleigh signal; the relatively low damage threshold of the Ronchi gratings makes the “standard” optical arrangement of SLIPI unsuited for the task. To solve this, we use an alternative approach to create the sinusoidal modulation based on a two-faceted glass component (see Fig. 2). Analogous to a cylindrical lens, passing through this optical component only affects the light in one lateral direction, effectively splitting the laser light beam into two beams. Both these are then focused into thin laser light sheets and

spatially overlapped at the measurement region where they, by interference, create the sinusoidal spatial modulation. The risk for damaging the optics is thereby minimized, however, it is important to make sure that the spatial coherence of the employed laser system is sufficient to form the interference pattern.

All tests were carried out in a laminar Bunsen-like CH_4/air flame ($\phi = 1.4$), having an adiabatic flame temperature of 1979 K. In an attempt to gradually increase the measurement complexity to demonstrate the filtering capabilities of SLIPI, three schemes were investigated; these will be referred to as Case 0, Case 1 and Case 2, and the respective configuration is shown in Fig. 2. In Case 0 – the most ideal situation – spurious light was shielded from the measurement region, and a black cloth, hanging 1 meter behind the burner (not shown in Fig. 2), was used to ensure a background-free condition. In Case 1 – the

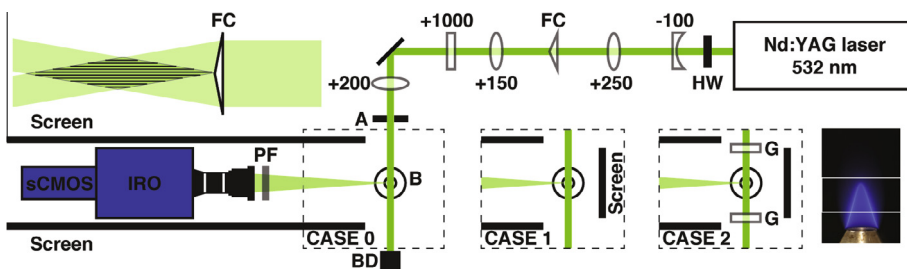


Fig. 2. Schematic view of the experimental setup and the three different measurement situations. Also included is an illustration of the principle for the two-faceted optical component. In the optical arrangement the laser light beam was first expanded to fully illuminate the two-faceted optical component (FC), which splits the beam into two. Two cylindrical lenses (+150 and +200 mm) were used to spatially overlap the two beams above the burner (B) and a third cylindrical lens (+1000 mm) was used to form both beams into laser light sheets. HW = half wave plate, A = aperture, BD = beam dump, PF = polarization filter, G = glass plate.

intermediate situation – a black screen was positioned 15 cm behind the burner in the field-of-view of the camera, thus generating moderately elevated levels of *diffuse* reflections. Case 2 – the most challenging measurement situation – attempts to mimic a scenario where optical ports are required. In addition to the screen in Case 1, two glass plates (30 cm apart) were positioned on either side of the burner, in turn generating high levels of both diffuse and sharp reflections and interferences.

To determine the improvements, in terms of evaluated temperature, realized by the SLIPI technique, the results were compared with those obtained using ordinary LRS, i.e., without an intensity-modulated laser light sheet. Alternating between the two illumination schemes was achieved by simply removing the two-faceted glass component and results acquired in this manner will be referred to as “conventional”. A pulsed frequency-doubled Nd:YAG laser (Quantel, Brilliant-b), delivering pulses of 532-nm wavelength at a repetition rate of 10 Hz (pulse duration ~ 10 ns) with a pulse energy of approximately 400 mJ, was used throughout the measurements. All LRS images were acquired using an intensified sCMOS camera (LaVision, Imager), equipped with a polarization filter, and the exposure time was set to 200 ns, during which the integrated chemiluminescence from the flame was negligible.

4. Results and discussions

Figures 3 and 4 show the results of the experiments for the three different measurement situations (Case 0–2). All temperature maps being presented here have been evaluated by dividing two images that were acquired with and without the flame ignited. Hence, the reference measurement was performed in air with an estimated gas temperature of 15 °C. Variations in Rayleigh scattering cross-sections in the flame were also taken into consideration, according to the procedure described in [23]. As can be seen in Fig. 4, the evaluated SLIPI-LRS temperatures in the product zone agree well with the adiabatic flame temperature, indicated by the dashed line.

The top row in Fig. 3 shows raw data images, recorded using the conventional LRS approach, where the strong contribution of stray light is clearly visible in Case 2. The dotted curve drawn near the top left corner highlights a sudden change in the background that will be transferred into undesired structures in the evaluated temperature (second row). Also noteworthy is that the influence of the screen in Case 1 is hardly observable in this image. The second row shows the evaluated temperatures, where the background – evaluated from the region just below the laser light sheet (indicated in Fig. 3) – was removed from the data.

The third row shows the corresponding SLIPI temperature images, where no background adjustments were applied, to illustrate the robustness of technique. The bottom row shows examples of single-shot temperature maps, acquired using SLIPI.

In Case 0, where the background is minimized experimentally, removing a constant offset is sufficient to reach satisfactory results, where symmetry and agreement with the adiabatic flame temperature (1979 K) are good indications of the fidelity of the measurement. The conventional and SLIPI temperature maps agree well, proving that the accuracy of LRS is not compromised when combined with the SLIPI technique. However, as background effects are increased, in Case 1, the results start to diverge and conventional LRS generates a less symmetric temperature realization, with a noticeable rise in the overall temperature by ~ 400 K (after compensating for the background offset). With no other modifications, these errors must be attributed to the added screen, giving rise to a weak *non-uniform* intensity offset. Attempting to compensate for such an offset is challenging and removing only a dc-component is insufficient; traces of stray light still present in the LRS image will lead to errors in the evaluated temperature and depending on its spatial distribution, stray light may either generate an increase or decrease in temperature. In the current case, stray light is appearing primarily in the low-temperature region of the flame, thus leading to an overestimated temperature field. At 2000 K, the observed increase of 400 K would correspond to non-uniform variations in the background of approximately $\pm 12\%$ around the average. As seen, by instead implementing SLIPI symmetry and absolute temperature is restored, which demonstrates that such interferences can be avoided. As the measurement complexity increases further, Case 2, the stray light problem becomes apparent even in the raw data image. Even though the glass plates on either side of the burner are kept well out of view, multiple reflections lead to lens flare and miscellaneous other interferences. As expected, applying conventional LRS to assess temperature in such a challenging environment leads to inaccurate results, in this case the evaluated temperature is well below the adiabatic flame temperature. Further, the temperature field is non-symmetric and characterized by large temperature gradients in the product zone. The temperature reading obtained by means of SLIPI shows none of the errors observed with conventional LRS and does, in contrast, manage to maintain both symmetry and absolute temperature. The somewhat reduced S/N observed in the SLIPI data obtained in Case 2 is probably due to shot noise, which is associated with the strong background. This increase in background is also expected to give rise to noise that appear at (or near) the spatial frequency of the modulated laser light sheet, but this needs to be

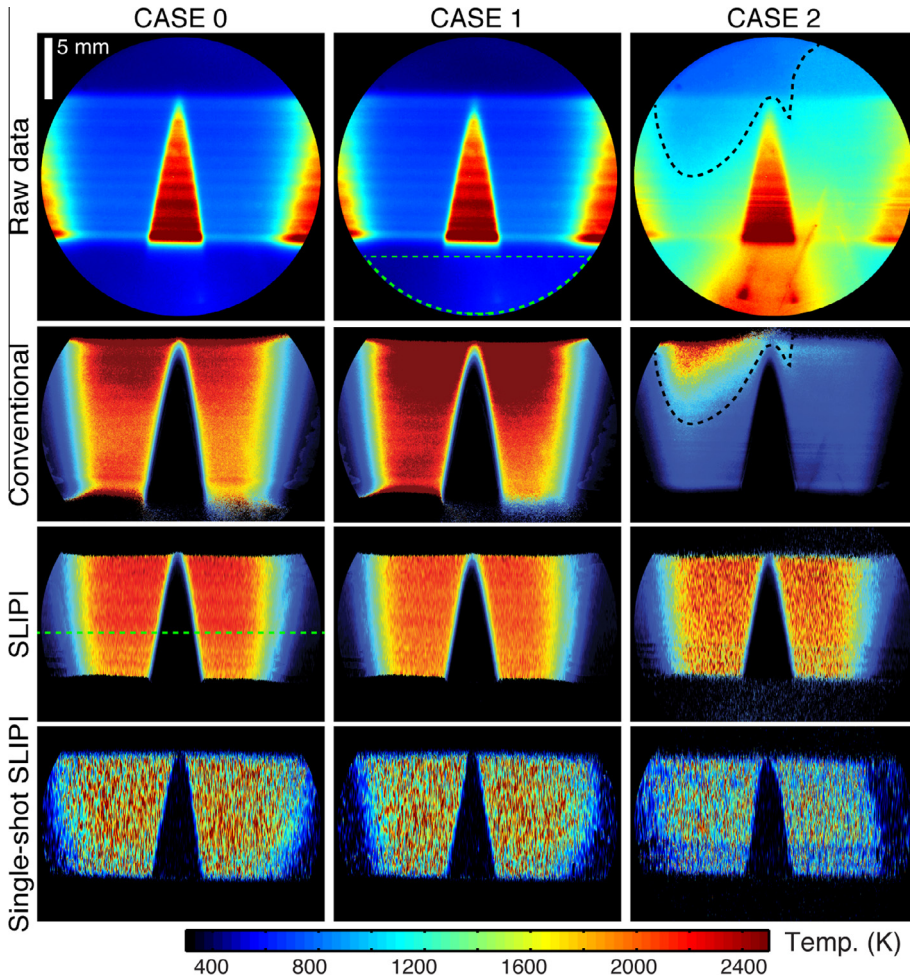


Fig. 3. (Top row) Conventional (raw data) LRS images. The dotted curve in the left corner highlights a sudden change in the background. The area marked by the green dashed line indicates the region over which the intensity background is evaluated. (Second row) Background-compensated LRS temperature fields, based on conventional data. (Third row) LRS temperature fields, based on averaged SLIPI data. The dashed vertical line indicates the region for the cross-sections in Fig. 4. (Bottom row) LRS temperature fields, based on single-shot SLIPI data. Note that no background evaluation routine was applied for the SLIPI results, as the technique automatically corrects for unwanted intensity contributions. The dashed vertical line indicates the region for the cross-sections in Fig. 4.

investigated further. This fact constitutes the ultimate limitation of the measurement concept. Yet regardless of a decreased S/N, the presented result conclusively illustrates the benefits of the proposed methodology and that the operating range of LRS thermometry can be increased by means of SLIPI.

Traditionally, LRS thermometry in flames requires pulsed lasers and gated detector systems to suppress chemiluminescence. This is essential to avoid biases toward lower temperatures, yet such equipment adds both measurement complexity and cost. In addition, MCP-equipped cameras often come with a reduced pixel density, compared to non-gated detectors. The SLIPI-LRS approach, however, opens up for rejection of che

miluminescence without image intensifier and, in principle, without a pulsed laser source. A demonstration of LRS thermometry, performed with a non-gated camera using the SLIPI concept, is shown in Fig. 5. In panel (a) an LRS image of a premixed Bunsen flame is captured using a non-gated sCMOS detector with an exposure time of 15 μ s. Notice how, in the high-temperature region of the flame, the chemiluminescence exceeds the Rayleigh signal, which, unless corrected for, will lead to an underestimation of the temperature in this zone. By processing the acquired image, panel (b), the chemiluminescence is suppressed, which permits an unbiased temperature evaluation, panel (c).

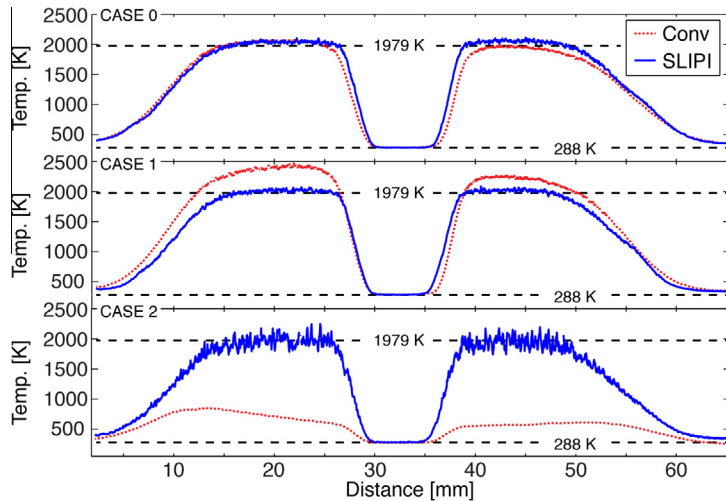


Fig. 4. Average temperature over the region indicated in Fig. 3. (Top graph) Case 0 – complete stray light shielding. The background-compensated conventional and SLIPI temperature fields agree well with the adiabatic flame temperature of 1979 K and both are symmetric around the inlet flow, as is expected. (Middle graph) Case 1 – low, yet not negligible, levels of stray light. The background leads to errors in the evaluated temperature in the conventional case, while no apparent change is observed in the SLIPI measurement. (Bottom graph) Case 2 – strong background interferences. Large variations in the background lead to unsatisfactory results with conventional LRS thermometry, whereas SLIPI still maintains both the symmetry and the value of the absolute temperature.

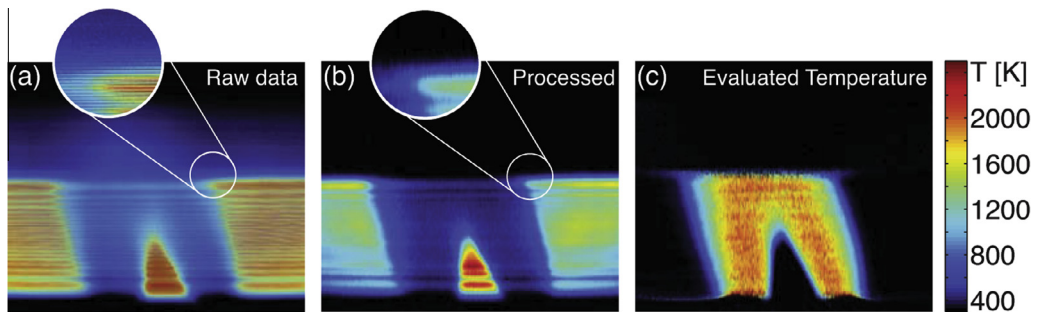


Fig. 5. Example of a SLIPI-LRS measurement of a premixed Bunsen flame, recorded using a non-gated sCMOS, having an exposure time of 15 μ s. (a) Chemiluminescence from the flame adds structure and intensity to the background that will create a bias to lower temperatures (see e.g., intensity contribution in the region above the laser sheet). (b) These unwanted effects are removed in the SLIPI post-processing, (c) in turn permitting stray light-free Rayleigh thermometry measurements with non-gated camera systems, thus reducing both cost and experimental complexity.

5. Summary and conclusion

In summary, an experimental methodology to mitigate the well-known stray light problem for laser-induced Rayleigh thermometry has been described and demonstrated. The proposed method employs an illumination scheme that differs from what is considered as “standard”. Instead of using an ordinary, top-hat laser light sheet, the intensity profile is spatially modulated with a sinusoidal shape, the purpose of which to mark the signal of interest and make it distinguishable from stray light. An LRS image acquired using such an approach will basically consist of two image

components; one carrying the superimposed spatial frequency, the other is characterized primarily by low spatial frequencies. By post-processing the data, the desired image component can easily be isolated and extracted, resulting in an image virtually free from interfering stray light.

The accuracy and reliability of the proposed method (SLIPI) has been investigated by gradually increasing the measurement complexity and thereby also the stray light contamination. Two-dimensional temperature images were acquired for each step using both conventional- and SLIPI LRS. Statements concerning the accuracy and reliability of each technique rely purely on the ability

to maintain stable results as stray light interference increases. From this perspective, the presented results conclusively illustrate the benefits of the SLIPI technology for Rayleigh thermometry, in both mild and relatively harsh measurement environments. Further investigations are, however, needed, to e.g. study eventual beam steering effects, determine sources of noise and understand how the optical setup can be optimized.

We firmly believe that SLIPI-LRS will be a valuable tool for 2-D thermometry in a great variety of experiments, particularly for measurements where the probe volume is surrounded by scattering surfaces and optical windows, which often is the case in practical combustion studies. Under such cumbersome conditions, traditional measures to reduce stray light are inadequate, which leads to both quantitative and qualitative temperature errors or, in the worst case, even prevents any temperature information from being extracted.

Acknowledgements

Finally, the authors wish to show their appreciation to the Linné Center within the Lund Laser Center (LLC), CECOST through the Swedish Energy Agency, and the ERC Advanced Grant DALDECS for financial support. We also thank Johan Zetterberg for important input regarding FRS.

References

- [1] G. Zizak, N. Omenetto, J.D. Winefordner, *Opt. Eng.* 23 (1984) 749–755.
- [2] J. Engström, J. Nygren, M. Aldén, C.F. Kaminski, *Opt. Lett.* 25 (2000) 1469–1471.
- [3] P.R. Medwell, Q.N. Chan, P.A.M. Kalt, Z.T. Alwahabi, B.B. Dally, G.J. Nathan, *Appl. Opt.* 48 (2009) 1237–1248.
- [4] J. Nygren, J. Engström, J. Walewski, C.F. Kaminski, M. Aldén, *Meas. Sci. Technol.* 12 (2001) 1294–1303.
- [5] N.M. Laurendeau, *Prog. Energy Combust. Sci.* 14 (1988) 147–170.
- [6] S. Roy, J.R. Gord, A.K. Patnaik, *Progr. Energy, Combust. Sci.* 36 (2010) 280–306.
- [7] A. Bohlin, B.D. Patterson, C.J. Klierer, *J. Chem. Phys.* 138 (2013) 081102.
- [8] S.W. Allison, G.T. Gillies, *Rev. Sci. Instrum.* 68 (1997) 2615.
- [9] M. Aldén, A. Omrane, M. Richter, G. Särner, *Prog. Energy Combust. Sci.* 37 (2010) 422–461.
- [10] A. Omrane, P. Petersson, M. Aldén, M.A. Linne, *Appl. Phys. B* 92 (2008) 99–102.
- [11] A. C. Eckbreth, *Laser Diagnostics for Combustion Temperature and Species*, 2nd ed. (Gordon & Breach, 1996).
- [12] I. Namer, R.W. Schefer, *Exp. Fluids* 3 (1985) 1–9.
- [13] V. Bergmann, W. Meier, D. Wolff, W. Stricker, *Appl. Phys. B* 66 (1998) 489–502.
- [14] G.S. Elliott, N. Glumac, C.D. Carter, *Meas. Sci. Technol.* 12 (2001) 452–466.
- [15] F.-Q. Zhao, H. Hiroysau, *Prog. Energy Combust.* 19 (1993) 447–485.
- [16] R.B. Miles, W.R. Lempert, J.N. Forkey, *Meas. Sci. Technol.* 12 (2001) R33–R51.
- [17] G. Tenti, C.D. Boley, R.C. Desai, *Can. J. Phys.* 52 (1974) 285–290.
- [18] E. Berrocal, E. Kristensson, M. Richter, M. Linne, M. Aldén, *Opt. Express* 16 (2008) 17870–17881.
- [19] M.A.A. Neil, R. Juskaitis, T. Wilson, *Opt. Lett.* 22 (1997) 1905–1907.
- [20] E. Berrocal, J. Johnsson, E. Kristensson, M. Aldén, *J. Eur. Opt. Soc. Rapid Publ.* 7 (2012) 12015.
- [21] E. Kristensson, J. Bood, M. Aldén, E. Nordström, J. Zhu, S. Huld, P.-E. Bengtsson, H. Nilsson, E. Berrocal, A. Ehn, *Opt. Express* 22 (2014) 7711–7721.
- [22] M.L. Meade, *J. Phys. E: Sci. Instrum.* 15 (1982) 395–403.
- [23] O. Johansson, J. Bood, B. Li, A. Ehn, Z.S. Li, Z.W. Sun, M. Jonsson, A.A. Konnov, M. Aldén, *Combust. Flame* 158 (2011) 1908–1919.